NASA Research Report No. 2

July 1963 29 p

The Physical Characteristics of Meteors

Gerald S. Hawkins and Richard B. Southworth

Harvard University

N64905

Smithsonian Institution Astrophysical Observatory, Cambridge (Mass.)

NASA Research Report No. 2

July 1963

The Physical Characteristics of Meteors

Gerald S. Hawkins[1], and Richard B. Southworth[2]

Introduction

In the early theories of the meteor process, the meteoroid was considered to be a solid body (Öpik 1937). Observations of photographic meteors (Jacchia 1955) showed that the meteoroid was not a solid object, but was a loose conglomeration of fragments that were shed continuously as the meteoroid penetrated the atmosphere. Progress has been made towards developing a new theory of the meteor process to allow for fragmentation (Öpik 1958), but the problem is complex. A typical meteor detected with a Super-Schmidt camera, visual magnitude +3, has a density of 0.4 gm cm^{-3}. During the luminous flight many thousands of fragments are shed and the total light and ionization produced is the sum of the contributions from all of these independent fragments. Some of the Super-Schmidt meteors, particularly those of low velocity and faint magnitude, suffered total fragmentation on meeting air resistance.

---

[1]Boston University, Boston, Mass; Smithsonian Astrophysical Observatory and Harvard College Observatory, Cambridge, Mass.

[2]Smithsonian Astrophysical Observatory, Cambridge, Mass.

The meteoroid completely disintegrated at the commencement of its luminous path and produced a cluster of independent particles. The crushing strength of this material is 10^4 dynes cm^{-2}, or approximately one third of a pound per square inch (McCrosky 1955). There are many objects amongst the very bright meteors that are solid pieces of stone and iron. The objects that produce fireballs are asteroidal fragments, whereas meteors with magnitudes between -5 and +5 are the debris ejected from comets. For example, a fireball as bright as the moon, visual magnitude -12, has a 95 percent probability of being a solid fragment (Hawkins 1959). However, fireballs of this brightness are a rarity and are not related to the average meteor. A progressive change therefore occurs in the physical characteristics of meteors as one goes from the brighter to the fainter objects. It is of interest to extend the observations to the regime of very faint meteors. This paper describes measurements that have been made by the Radio Meteor Project to a limiting visual magnitude of +10.

Observational Data

A six-station radar system has been operated at Havana, Illinois, at a frequency of 40.92 mcs (Hawkins 1963). The Fresnel pattern of the meteor is measured with a digitized film viewer, and the data are processed by a 7090 IBM Digital machine. The system measures velocity with a precision of about $\pm \frac{1}{2}$ km sec^{-1}, and the electron density is measured along the trail at six positions or less. The total ionization is calculated by integrating the ionization curve, and the magnitude of the meteor is derived from the theoretical ionizing efficiency (Lazarus and Hawkins 1963). The mass of an individual meteor may have an uncertainty

of a factor of 2, largely because of uncertainty in the position of the meteor trail within the antenna pattern. There may also be a systematic error in all masses because of the present uncertainty in the ionizing efficiency. It should be noted that the adopted luminous efficiency gives a meteor of zero visual magnitude a mass of 1 gm (Whipple 1963), and the ionizing efficiency gives a mass of 5 gm for the same meteor. It is impossible to reduce this discrepancy without experimental determinations of the ionizing efficiency, and at the present time there may be a systematic error of approximately a factor of five in the mass scale of either method.

Approximately 3,500 meteors have been observed and reduced with the equipment. Under certain restrictive conditions it is possible to measure the height of some of these meteors. When the radiant of the meteor is in such a position that the meteor trail is aligned with the direction of the transmitting antenna, then the echo line (Clegg 1948) passes through the antenna pattern at almost constant altitude. This geometry is illustrated in Fig. 1 where the sensitivity contours of the transmitting antenna are shown, together with a locus of possible echoing points for given zenith angles of the radiant. Since the zenith angle of the radiant is measured by the system, the altitude of the echo point is known and the height can be determined from a knowledge of the range. The estimated error in this height determination is ± 4 km, accurate enough for statistical purposes.

The physical data for 327 meteors are listed in Table 1. The sample represents all meteors for which heights could be obtained during the period from November 1961 to March 1962. Apart from the radiant selection mentioned in the previous section, these meteors are a random sample. Most of the meteors do not belong to the major streams, and Geminid, Quadrantid and other stream meteors are marked in the Table. The time of appearance of the meteor is given in C.S.T.

The maximum magnitude was derived from the maximum electron line density g_{max} per meter by use of the relation

$$M_{max} = 40 - 2.5 \log_{10} g_{max} \quad . \tag{1}$$

This magnitude corresponds approximately to the visual magnitude of the meteor, although to be precise it must be called a radio magnitude. We may convert to visual magnitude by adding a small correction, δM, which may be called a velocity index (Hawkins 1956). A revised value (McKinley 1961) of the velocity index is given in Table 2.

Table 2

Velocity Index (Visual = Radio + Index)

v km sec^{-1}	10	20	30	40	50	60
Index	-1.5	-0.7	-0.3	0.0	+0.2	+0.4

It can be seen that the two magnitude scales coincide at a velocity of 40 km/sec.

The original mass of the meteor, m_∞, has been determined from the relation

$$m_\infty = 1.86 \times 10^{-14}\ Q\ v^{-3.4} \tag{2}$$

where Q is the total number of electrons in the trail, v is the mean velocity of the meteor in km sec^{-1} and the mass is given in gm.

The density given in Table 1 must be regarded as a nominal density, because it is impossible to determine the original density of the meteoroid before total fragmentation occurred. This nominal density has been obtained by applying the drag equation, on the assumption that the meteoroid is a single body and that the product $\Gamma A = 1.0$;

$$\rho_m = \left(\frac{\rho_a v^2}{|\dot{v}|}\right)^{3/2} \left(\frac{m_\infty}{2}\right)^{-\frac{1}{2}} \tag{3}$$

The deceleration $\dot{v}$ is in units of km sec^{-2}, and ρ_a is the atmospheric density corresponding to the mean height of the trail. The nominal density must not be taken as that of the meteoroid before entering the atmosphere since there is no quantitative connection between these values. The nominal density, however, is a useful parameter for estimating the number and size of the fragments produced by the meteoroid. If we assume that the meteor breaks up into N identical fragments of density ρ_o, then a re-examination of equation (3) shows that

$$N = \left(\frac{\rho_o}{\rho_m}\right)^2 \tag{4}$$

If one assumes that the fragments are spherical with radius s then the radius is given by the expression

$$s = 0.62\ m_{\infty}^{1/3}\ \rho_m^{2/3}\ \rho_o^{-1}\ . \tag{5}$$

In fact, the fragments will be unequal in size and only the larger ones will be observed. Hence, N is a lower limit to the number of fragments, and s is an upper limit to the average radius.

The quantity σ is the deceleration parameter used in photographic studies of meteors. It is defined by the relation

$$\sigma = \frac{\dot{m}}{m\,v\,\dot{v}} \tag{6}$$

and in the single body theory it is equal to $\Lambda/2\ \Gamma\zeta$, where Λ is the heat-transfer coefficient, Γ is the drag coefficient, and ζ is the energy required to ablate one gm of the meteoroid. In the single body theory, σ is easy to evaluate from known physical constants. For most materials the value is close to 10^{-12} cgs units. For a meteoroid that is shedding fragments or breaking up, the deceleration parameter does not have such a clear meaning, but it is a useful quantity for studying the behavior of the meteoroid.

An appropriate ionization curve could be deduced for a majority of the meteors in the sample. The "beginning" and "end" heights of these meteors are the extrapolated heights at which the ionization was just detectable, and the "maximum" heights are at the maxima of the ionization curves. The "beginning" height adopted for a meteor without an adequate

ionization curve is 0.8 km above the highest point detected in the Fresnel patterns, and the "end" height is 0.8 km below the lowest point detected. The value 0.8 km is equal to 0.4 of the average spacing between the echo points from two adjoining stations. The adopted "maximum" height for these meteors is the mean of the beginning and the end.

The height of meteors is tabulated as a function of velocity and magnitude in Table 3. The blanks in the table, of course, represent velocity and magnitude classes for which no meteors were observed. Table 4 gives the average heights for all but seven of the meteors as a function of the measured velocity. These seven meteors were observed with low (25 km) transmitter power, and are omitted from Table 4 in order to have a more homogeneous sample.

Table 4

Height as a function of velocity

v	10-15	15-20	20-25	25-30	30-35	35-40	40-45	45-50	50-55	55-60 km/sec
H_{beg}	88.8	94.0	90.6	93.5	95.3	96.5	101.2	98.5	93.6	95.8
H_{max}	84.7	90.3	86.7	89.2	91.0	92.3	97.1	94.9	90.4	91.8
H_{end}	81.7	86.7	83.1	85.3	87.0	88.3	92.6	90.8	87.6	88.0
H_{mean}	85.2	90.3	86.8	89.3	91.1	92.4	97.0	94.7	90.5	91.9
Number	2	9	39	68	100	68	21	9	2	2

In these tables the data for shower meteors have been included because we could detect no difference between the data for stream and for sporadic meteors.

Of the 327 meteors, 78 show decelerations that are less than two thirds of their standard errors. These meteors represent, in general, poor quality observations and have been rejected from the deceleration analysis. In Table 5 we give the deceleration parameter, σ , and the nominal density, ρ_m, for various classes of velocity and magnitude. Finally, in Table 6 we give the deceleration, $-\dot{v}$, as a function of velocity.

Discussion

From the foregoing data we have derived the following approximate correlations for height, deceleration, deceleration parameter and nominal density:

$$H_{mean} = 91 + 18 \log_{10} (v/30) - 2.7 (M_{max} - 8.5) \tag{7}$$

$$\log_{10} |\dot{v}| = 1.2 + 1.9 \log_{10} (v/30) + 0.15 (M_{max} - 8.5) \tag{8}$$

$$\log_{10}\sigma = -11.6 - 2.2 \log_{10} (v/30) - 0.2 (M_{max} - 8.5) \tag{9}$$

$$\log_{10}\rho_m = -1.3 - 1.2 \log (v/30) + 0.1:(M_{max} - 8.5) \tag{10}$$

$$\log_{10}\rho_m = -1.42 + 0.07 (\log_{10} m_\infty + 2.5) \ . \tag{11}$$

The velocity is in units of km sec^{-1} and M_{max} is a radio magnitude.

The most significant result in these correlations is that in equation (7), the dependence of mean height on magnitude. The theoretical relationship between H and v depends upon the ionizing probability β. If the value for β is taken from Lazarus and Hawkins (1963) and used in the single body theory, then equation (7-26) of McKinley (1961) becomes

$$H_{max} = \text{constant} + 41 \log_{10} v + 1.8 M_{max} . \qquad (12)$$

For the present purpose the difference between H_{mean} and H_{max} may be ignored and we may compare equations (7) and (12) directly. The experimental values clearly differ considerably from the predictions of the single body theory. In particular, the height is found to depend less strongly on velocity as indicated by the theory. The height decreases for fainter meteors instead of increasing as the theory predicts.

It is interesting to note that we can interpret the observational data in terms of the deceleration parameter σ, and the nominal density ρ_m, both of which are related to the physical characteristics of the meteors. If σ and ρ_m are treated as variables, then one must add extra terms to equation (12). This equation becomes

$$H_{max} = \text{constant} + 41 \log_{10} v + 1.8 M_{max} + 12 \log_{10} \sigma - 8 \log_{10} \rho_m . \qquad (13)$$

If we now substitute the observed correlations as given by equations (9) and (10) into the theoretical equation (13), then the height-velocity relationship becomes

$$H_{max} = \text{constant} + 24 \log_{10} v - 1.4 M_{max} . \qquad (14)$$

This equation is in fair agreement with equation (7), and shows that the theory must be modified to account for the differences in physical characteristics of meteors as a function of velocity and magnitude.

The mean heights measured in this program may be compared with those obtained from similar radio echo observations. Evans (1955) has determined the height of meteors as a function of velocity, using a double antenna system which permitted the measurement of the angle of elevation of the echo point. The mean characteristic heights determined by Evans are represented by the line in Figure 2. The characteristic height is the height corrected so as to apply to the point of maximum ionization of the faintest meteor detected by his equipment. It is closely comparable to the "mean" height quoted in this experiment. The limiting magnitude of Evan's equipment was +6.5, some three magnitudes brighter than that of the Radio Meteor Project. The two sets of observations are in fair agreement, but neither is consistant with the curve corresponding to the single body theory. This discrepancy is accounted for in terms of the physical characteristics of the meteors as shown in the derivation of equation (14).

That the height of faint meteors are anomalous is shown further in Figure 3, where the height of maximum ionization (or maximum light) is plotted as a function of magnitude. The photographic meteors tend to follow the single body theory remarkably well, but at magnitude +3, meteors begin to penetrate the atmosphere to greater depths than the theory predicts. The results of the Radio Meteor Project have been divided into two groups having mean magnitudes of +8.7 and +9.3, respectively. At these faint magnitudes the meteor trails are some 10 km lower than the expected height. This anomalous behavior is indeed fortunate for radar programs,

for if the trails were occurring at the predicted heights, then the echoes would be distorted by the effects of diffusion in the atmosphere. The height anomaly is the primary cause of the high quality Fresnel patterns obtained in the Radio Meteor Project. The height anomaly also minimizes the selection effects which would otherwise be introduced by the diffusion ceiling.

The height-magnitude curve in Figure 3 can be interpreted in the following manner. Bright meteors continuously shed fragments during their passage through the atmosphere and thus behave to some extent as a single body. The larger meteoroids are extremely fragile and particles are dislodged at an early stage in the trajectory. On the other hand, the fainter meteors at magnitude +9 do not shed fragments, but disintegrate completely at the beginning of the trajectory. Super-Schmidt meteors at magnitude +3 represent a transition region where some of the meteors are showing total fragmentation at the beginning of the trajectory. This may be due to the fact that the meteoroids are so small that the shedding of a layer of fragments is tantamount to break-up of the body. The majority of the faint radio meteors show total fragmentation, as will be shown in the discussion of σ. These meteors occur at approximately the same height as the Super-Schmidt meteors and therefore exhibit the same crushing strength. There are indications, however, that the crushing strength may increase slightly for the small objects, because the mean height of meteors at magnitude +9 is approximately 1 km lower than meteors at +8.

Further confirmation of our interpretation of the physical characteristics of meteors is given by the deceleration parameter σ. The correlation shown in equation (9) is weak, but it indicates that σ reaches the value for a single body at the limiting magnitude of the present equipment. At a velocity of 30 km sec^{-1}, for example, $\sigma = 10^{-12}$ at a magnitude of +10.5. At this point we are presumably dealing either with a single particle or with a cluster of independent particles.

We can distinguish between a cluster and a single particle by referring to the nominal density ρ_m. In every group, the average density is considerably less than that for a solid fragment of stone or iron. We may take $\rho_o = 2.5$, while the average value of $\log_{10} \rho_m$ is -1.42 as given by equation (11). The average number of particles is then given by equation (4) as approximately 4,000. The average radius s is given by equation (5) and is 40 microns. The mass of an individual fragment is approximately 10^{-6} gm.

It is surprising to note that the number of fragments is almost independent of the mass of the meteoroid in the radio meteor sample. Equation (11) shows only a slight correlation between the nominal density and the mass of the meteoroid. Thus, it seems that several thousand fragments are observed whether the meteor is large or small. This may indicate that the fragments produced by disintegration of a meteoroid are unequal in size. If there is a size distribution amongst the fragments then it is conceivable that the observations will detect about a thousand of the largest fragments and that there may be many more smaller fragments that are not contributing to the total ionization.

There are also indications that the high velocity meteors are smashed more thoroughly than slow meteors. Equation (10) shows that ρ_m decreases with velocity and hence that the number of fragments, N, increases as v^2.

References

Clegg, J. A., 1948, Phil. Mag. 39, 577.

Evans, S., 1955, Suppl. Jour. Atmos. Ten. Phys., 2, 86.

Hawkins, G. S., 1956, Ast.phys. Jour. 124, 311.

Hawkins, G. S., 1959, Ast. Jour. 64, 450.

Hawkins, G. S., 1963, Smith. Cont. Ap. 7, 53.

Jacchia, L. G., 1955, Ast.phys. Jour. 121, 521.

Lazarus, D. M., and Hawkins, G. S., 1963, Smith. Cont. Ap. 7, 221.

McCrosky, R. E., 1955, Ast. Jour. 60, 170.

McKinley, D. W. R., 1961, Meteor Science and Engineering. McGraw-Hill New York.

Öpik, E. J., 1937, Pub. Ast. Obs. Tartu, 29 No. 5.

Öpik, E. J., 1958, Physics of Meteor Flight in the Atmosphere, Interscience Publishers Inc., New York.

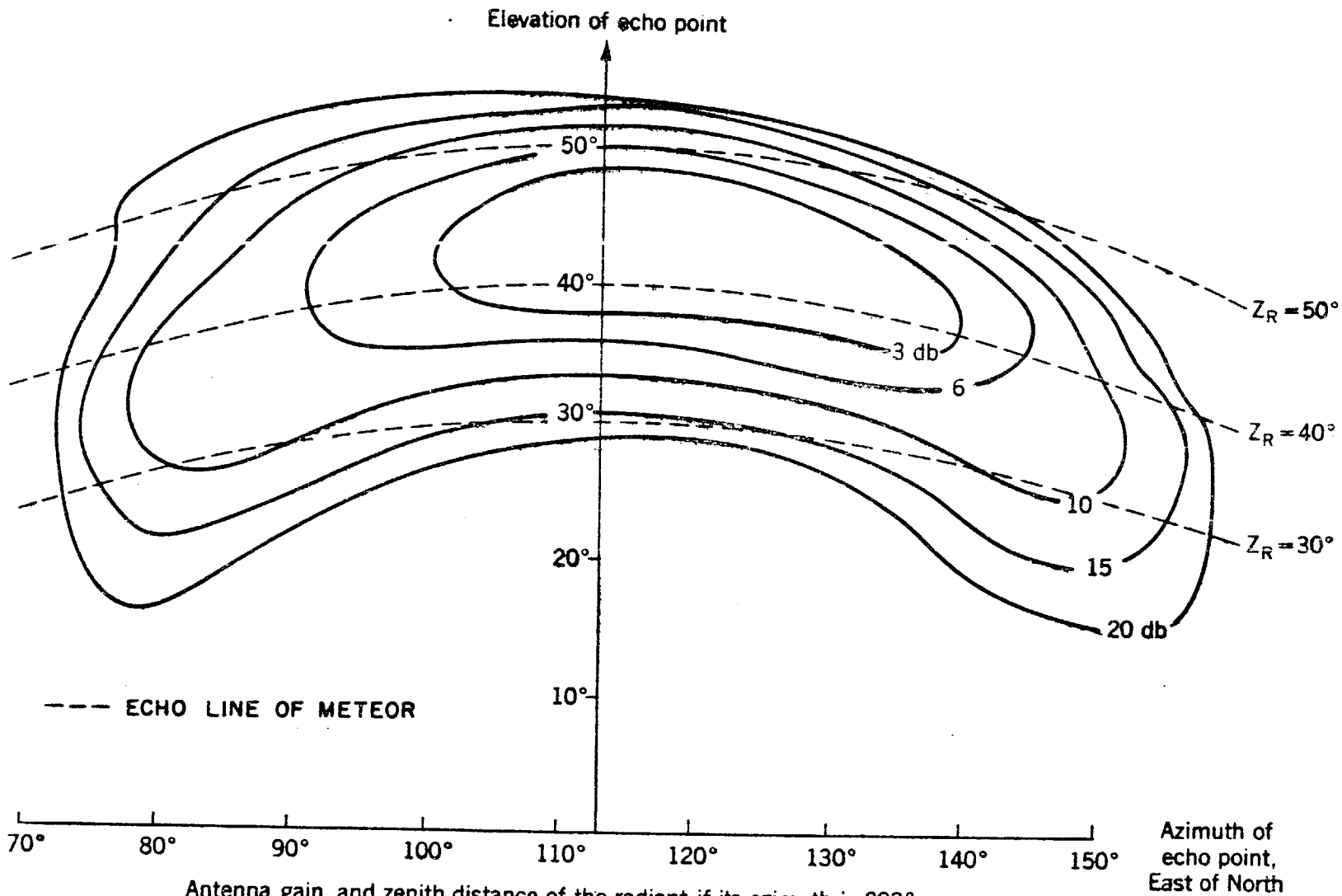

Antenna gain, and zenith distance of the radiant if its azimuth is 293°.

FIGURE 1

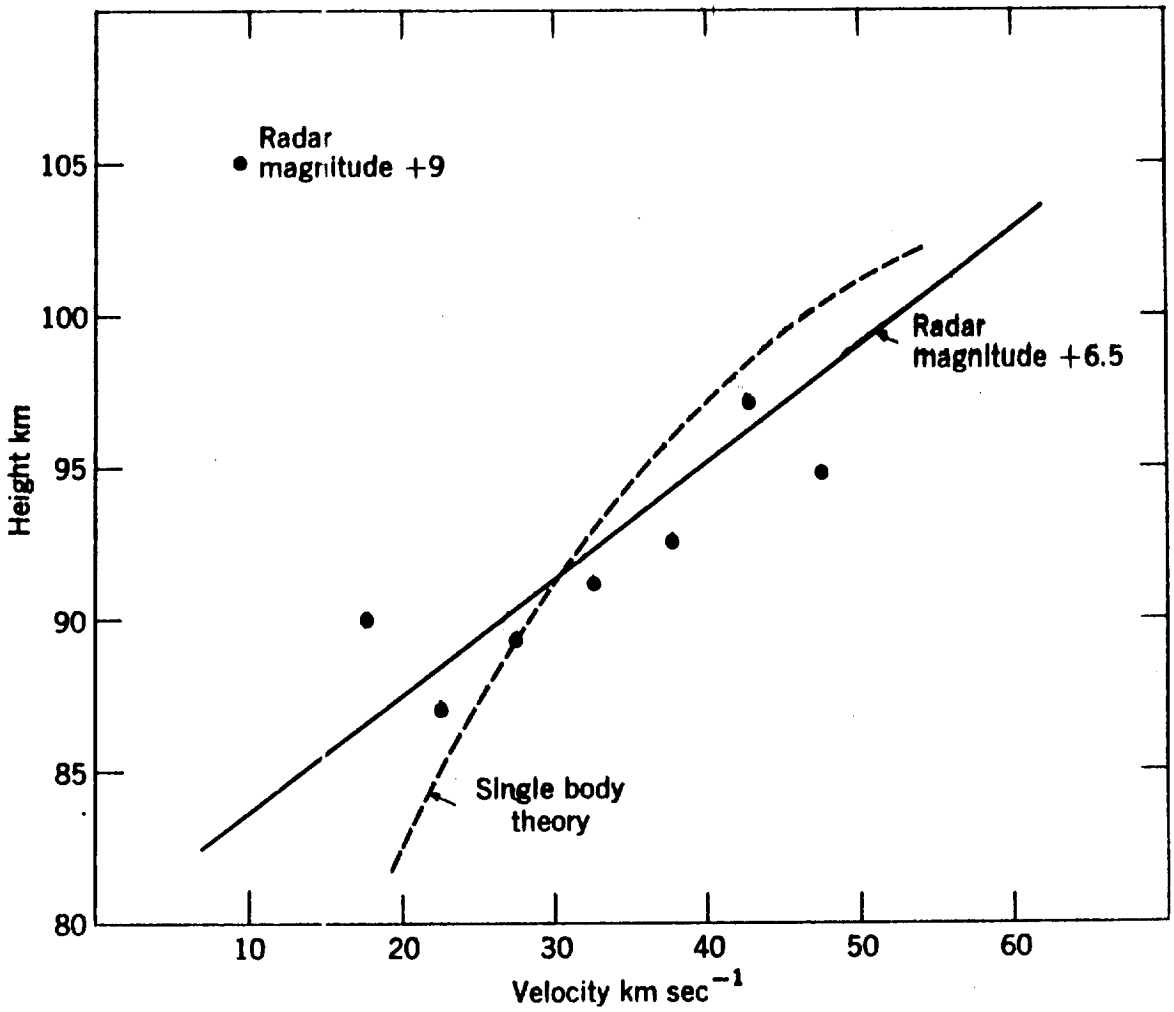

MEAN HEIGHT VERSUS VELOCITY
FIGURE 2

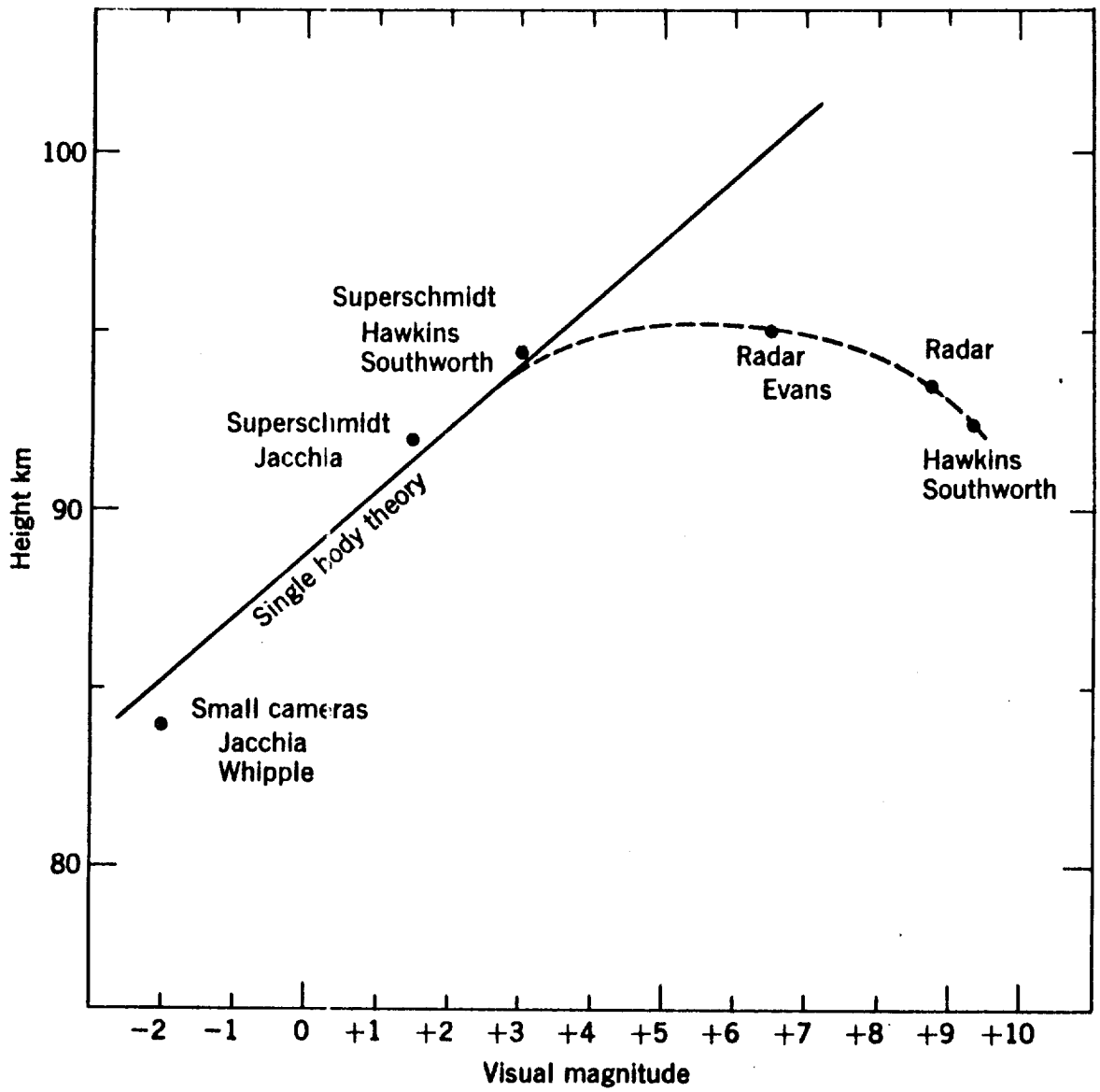

METEOR HEIGHT AT V = 40 KM SEC^{-1}
FIGURE 3

TABLE 1 - Height and other related data for 327 meteors

DATA FOR 327 METEORS

COLUMN IDENTIFICATIONS

1 NUMBER
2 DATE 1961-2 (CENTRAL STANDARD TIME)
3 HOUR AND MINUTE (CENTRAL STANDARD TIME)
4 SHOWER G = GEMINID Q = QUADRANTID
5 NUMBER OF STATIONS RECORDING THE METEOR
6 TRANSMITTER POWER A = 25 KW B = 700-1200 KW C = 1500-2500 KW
7 MAXIMUM RADIO MAGNITUDE
8 RISE ABOVE NOISE LEVEL = (NOISE MAGNITUDE) MINUS (MAXIMUM MAGNITUDE)
9 COSINE OF ZENITH DISTANCE OF RADIANT
10,11,12 HEIGHTS ABOVE SEA-LEVEL (KM) THERE IS A STANDARD DEVIATION OF 4 KM IN THE HEIGHT OF EACH METEOR. IN ADDITION, STARRED HEIGHTS ARE NOT WELL DETERMINED BY THE IONIZATION CURVE.
13 MEAN VELOCITY (KM/SEC)
14 MEAN DECELERATION (KM/SEC/SEC)
15 STANDARD DEVIATION OF DECELERATION
16 LOG10 OF EXTRA-ATMOSPHERIC MASS (GM)
17 LOG10 OF NOMINAL DENSITY (CGS)
18 LOG10 OF SIGMA (CGS)

NO	DATE 196-	TIME CST				MAX MAGN	MAGN RISE	COS Z	BEG HT	MAX HT	END HT	V	VDOT	ER-ROR	LOG MASS	LOG DENS	LOG SIGMA
1	2	3	4	5	6	7	8	9	10	11	12	13	14	15	16	17	18
3003	27NO1	3 4		3	A	7.3	1.0	.75	108.1*	102.2	97.3*	27.9	-.30	4.4	-1.6	-0.8	-10.2
3004	27NO1	321		3	A	6.5	1.8	.77	111.1*	107.5	101.0*	32.6	-.91	4.7	-1.5	-1.6	-10.6
3005	27NO1	337		3	A	7.2	1.4	.74	92.9*	89.9*	87.0*	27.4	-12.	4.7	-1.8	-1.6	-11.5
3008	27NO1	347		3	A	6.7	1.5	.83	97.4	94.4	91.9	33.6	24.	16.	-2.0	-2.3	-11.7
3013	27NO1	358		3	A	5.7	2.5	.83	96.9	94.2*	92.5	26.1	-4.4	16.	-1.3	-1.8	-10.9
3020	27NO1	435		6	A	6.5	1.6	.82	110.9*	104.0	96.1	43.5	-16.	6.0	-1.8	-2.7	-12.0
3026	27NO1	5 4		3	A	6.4	1.9	.80	100.3*	97.5*	94.7*	34.2	-9.4	21.	-1.8	-2.0	-11.3
3081	4DE1	5 7		3	B	8.3	1.7	.87	88.9*	86.0*	83.1*	34.5	50.	62.	-2.6	-1.3	-12.0
3082	4DE1	522G		4	B	8.0	2.2	.76	99.5	94.2	88.9	34.2	11.	7.5	-2.2	-1.6	-11.7
3083	4DE1	525G		3	B	7.7	2.3	.80	104.3*	101.2*	98.0*	32.9	-13.	9.5	-2.3	-2.5	-11.5
3085	4DE1	532		4	B	7.7	2.5	.83	96.0*	91.7*	87.5*	37.4	8.3	5.0	-2.3	-0.8	-11.5
3088	4DE1	612		4	B	8.2	2.0	.83	91.0	86.3	81.6	29.5	12.	1.3	-2.1	-0.9	-11.6
3095	4DE1	628		3	B	8.9	1.4	.74	100.8*	95.7	92.8*	27.7	15.	15.	-2.3	-2.3	-11.7
3096	4DE1	634G		4	B	8.5	2.1	.73	87.1	82.6	78.5	30.4	8.4	1.9	-2.3	-0.2	-11.5
3099	4DE1	640		4	B	8.1	2.4	.76	92.2*	88.1*	84.0*	24.7	9.4	.75	-1.8	-1.2	-11.5
3104	4DE1	649		4	B	8.1	2.0	.81	93.7	87.2	84.1*	33.1	6.4	2.1	-2.2	-0.7	-11.4
3152	6DE1	458		4	B	8.2	2.5	.75	96.7	89.5	88.0*	32.4	.74	5.5	-2.2	0.3	-10.5
3154	6DE1	459		4	B	9.0	1.4	.81	101.7*	96.6	91.3	44.4	48.	21.	-3.0	-2.1	-12.3
3162	6DE1	519		4	B	8.0	2.5	.73	108.8*	100.5*	97.7*	38.7	3.9	11.	-2.3	-1.8	-11.3
3163	6DE1	527G		3	B	8.8	1.6	.80	98.0*	95.2*	92.5*	32.4	21.	12.	-2.7	-1.9	-11.7
3167	6DE1	544G		4	B	9.2	1.5	.74	97.5*	90.2	87.6*	34.7	27.	4.4	-2.7	-1.6	-12.1
3170	6DE1	551G		3	B	9.1	1.6	.73	97.1	94.0	91.7*	34.3	19.	20.	-2.9	-1.7	-11.7
3172	6DE1	552G		4	B	9.1	1.4	.81	93.1*	85.7	82.6*	23.1	9.7	3.7	-2.1	-1.3	-11.6
3173	6DE1	559		4	B	8.0	2.2	.89	93.6*	89.8	84.5	49.5	59.	62.	-2.8	-1.1	-12.3
3177	6DE1	648		3	B	7.6	2.5	.87	94.9	92.1*	90.7	31.1	13.	20.	-2.4	-1.5	-11.3
3190	7DE1	5 9G		3	B	9.1	1.5	.80	88.4*	85.7*	82.9*	35.3	6.2	22.	-3.0	0.3	-11.2
3204	7DE1	558G		4	B	8.3	2.5	.69	94.8*	90.6*	86.5*	34.9	9.0	7.6	-2.4	-0.8	-11.6
3205	7DE1	560		4	B	8.0	2.4	.80	102.4*	94.6	92.4*	28.5	20.	13.	-2.0	-2.6	-11.9
3220	7DE1	7 5		4	B	9.3	1.2	.81	97.6*	93.3*	89.1*	29.3	31.	8.7	-2.6	-2.1	-12.0
3234	7DE1	912		5	B	8.1	2.1	.87	99.9*	94.8*	89.7*	27.3	-8.1	6.3	-1.9	-1.8	-11.5

NO	DATE 196-	TIME CST				MAX MAGN	MAGN RISE	COS Z	BEG HT	MAX HT	END HT	V	VDOT	ER-ROR	LOG MASS	LOG DENS	LOG SIGMA
1	2	3	4	5	6	7	8	9	10	11	12	13	14	15	16	17	18
3246	8DE1	347	5	B		8.3	1.9	.85	99.6*	92.0	86.8*	35.4	16.	8.1	-2.3	-1.6	-11.9
3254	8DE1	412	3	B		8.3	2.1	.84	92.7*	89.6*	86.4*	27.9	8.5	3.0	-2.2	-1.1	-11.3
3255	8DE1	413	4	B		9.3	1.5	.79	84.7*	80.9*	77.2*	20.6	23.	6.6	-2.1	-1.0	-11.9
3258	8DE1	438G	3	B		8.8	1.5	.82	98.9*	96.0*	93.2*	30.5	4.2	25.	-2.6	-1.0	-11.0
3260	8DE1	445	3	B		8.5	1.7	.84	102.7*	99.5*	96.3*	33.8	15.	15.	-2.6	-2.1	-11.6
3275	8DE1	535	3	B		8.2	2.5	.69	100.2	97.0*	93.8	29.3	35.	6.7	-2.2	-2.8	-12.0
3280	8DE1	546	3	B		9.2	1.6	.71	92.9*	90.1*	87.3*	27.7	23.	7.7	-2.6	-1.6	-11.8
3289	8DE1	627	3	B		8.7	2.0	.75	95.0	92.3	90.2	32.1	28.	9.7	-2.7	-1.8	-11.8
3314	9DE1	410	3	B		8.2	2.0	.83	99.6*	96.5*	93.4*	33.7	21.	8.4	-2.5	-2.1	-11.7
3315	9DE1	412	3	B		8.1	2.5	.75	93.1	90.4*	88.1	24.2	12.	3.2	-2.0	-1.7	-11.4
3318	9DE1	440	4	B		8.2	2.0	.85	95.5*	91.1*	86.6*	31.9	15.	3.2	-2.3	-1.4	-11.7
3337	9DE1	510G	4	B		8.6	1.8	.79	96.9*	92.3*	87.6*	31.5	16.	2.5	-2.4	-1.6	-11.8
3341	9DE1	558G	4	B		8.9	1.8	.69	95.2	88.5	86.1*	31.8	16.	3.4	-2.5	-1.3	-11.9
3343	9DE1	6 0	4	B		8.1	2.4	.76	99.3*	93.6	88.7*	42.2	-5.4	4.3	-2.5	-0.6	-11.4
3345	9DE1	6 1G	4	B		9.2	1.5	.71	94.8*	90.6*	86.4*	32.1	6.4	8.6	-2.6	-0.6	-11.4
3370	9DE1	720	4	B		8.1	2.3	.81	97.1*	94.7	85.6*	45.2	39.	5.0	-2.6	-1.5	-12.3
3413	10DE1	510	3	B		7.7	2.5	.86	95.2*	92.0*	88.9*	45.5	-11.	24.	-2.8	-0.7	-11.4
3416	10DE1	515	4	B		8.8	1.7	.70	102.9	98.8	95.0	32.7	22.	3.7	-2.5	-2.5	-11.9
3423	10DE1	517	4	B		8.8	1.4	.83	99.3	94.3	89.3	26.8	10.	3.4	-2.2	-1.9	-11.6
3429	10DE1	523	4	B		8.2	2.5	.72	97.1*	93.1*	89.2*	23.5	5.5	1.2	-1.8	-1.6	-11.3
3433	10DE1	526G	4	B		8.4	2.2	.76	94.7	90.7	87.2	36.7	10.	6.3	-2.6	-0.8	-11.5
3438	10DE1	539G	4	B		8.8	1.9	.71	100.3*	96.1*	91.9*	34.5	26.	3.7	-2.6	-2.1	-12.0
3439	10DE1	540G	3	B		9.3	1.4	.75	92.0*	89.0*	86.1*	33.3	27.	5.9	-2.9	-1.2	-11.8
3443	10DE1	545G	3	B		8.9	1.7	.74	91.9*	89.0*	86.0*	33.1	18.	5.8	-2.7	-1.0	-11.7
3445	10DE1	548G	4	B		9.8	0.8	.72	101.9*	97.9*	93.8*	32.4	28.	8.6	-2.9	-2.3	-12.0
3452	10DE1	556	5	B		8.4	2.0	.81	95.4	89.7	84.0	36.6	14.	4.3	-2.4	-0.9	-11.8
3453	10DE1	558G	3	B		9.0	1.6	.76	92.7	88.8	86.1*	34.9	5.5	9.5	-2.8	-0.2	-11.2
3455	10DE1	559	5	B		9.3	1.6	.66	92.8*	87.9*	82.9*	32.2	19.	5.2	-2.6	-1.0	-12.0
3470	10DE1	7 3	3	B		8.3	1.9	.89	86.6*	83.5*	80.3*	48.6	-18.	18.	-3.1	0.3	-11.6
3483	10DE1	8 6	3	B		8.9	1.4	.86	89.2*	86.2*	83.2*	24.7	5.3	10.	-2.3	-0.4	-11.1
3523	11DE1	460	4	B		9.1	1.5	.79	94.0*	88.2	83.3*	34.4	22.	4.6	-2.6	-1.2	-12.0
3525	11DE1	5 3	4	B		8.0	2.5	.72	114.6*	110.5*	106.3*	36.6	20.	3.2	-2.3	-3.5	-11.9
3555	11DE1	537G	4	B		8.7	1.8	.74	103.9	97.2	93.8*	34.2	5.8	6.6	-2.5	-1.7	-11.4
3556	11DE1	539	3	B		8.6	1.6	.88	92.2*	89.0*	85.9*	38.0	20.	12.	-2.9	-0.8	-11.7
3557	11DE1	542G	4	B		8.4	2.5	.71	92.5	88.4	84.3*	30.6	49.	15.	-2.2	-1.9	-12.3
3559	11DE1	544G	4	B		8.6	2.1	.75	91.5*	84.7	80.8*	31.8	19.	1.9	-2.3	-1.0	-12.0
3560	11DE1	545	4	B		8.9	1.5	.80	99.8*	95.8*	91.7*	27.2	14.	3.1	-2.4	-2.0	-11.7
3562	11DE1	552G	4	B		8.2	2.4	.72	103.9*	99.8*	95.7*	34.1	9.5	3.6	-2.3	-2.0	-11.5
3563	11DE1	556G	3	B		8.3	2.5	.71	89.6	86.2*	83.8*	34.7	-2.3	5.2	-2.6	0.5	-10.8
3564	11DE1	557	4	B		8.3	2.0	.82	102.3	95.6	92.6*	31.0	-5.1	5.1	-2.2	-1.6	-11.3
3573	11DE1	638	4	B		9.2	1.4	.78	95.5	90.0	84.9*	27.6	.95	3.4	-2.3	0.3	-10.6
3575	11DE1	645	4	B		8.3	2.2	.78	95.0	90.5	86.6*	36.8	22.	6.9	-2.5	-1.4	-11.9
3586	11DE1	712	4	B		7.9	2.5	.84	93.8*	89.2*	84.6*	56.6	12.	22.	-3.0	0.0	-11.6
3604	11DE1	811	4	B		9.0	1.5	.84	91.8*	84.4	79.3*	28.6	18.	1.8	-2.3	-0.9	-11.9
3610	11DE1	820	4	B		7.9	2.5	.83	96.0*	91.5*	86.9*	48.8	9.1	10.	-2.7	-0.4	-11.5
3639	13DE1	531G	3	B		8.8	2.0	.76	82.7*	79.9	76.1	30.2	40.	21.	-2.5	-0.6	-12.1
3641	13DE1	531	3	B		8.4	2.3	.83	76.5*	73.4*	70.4*	28.8	70.	11.	-2.4	-0.5	-12.2
3642	13DE1	532	3	B		9.3	1.4	.80	81.8*	78.7*	75.6*	21.0	8.6	2.8	-2.2	-0.2	-11.3
3649	13DE1	540	3	B		9.1	1.4	.83	86.8*	83.7*	80.5*	28.9	7.7	6.3	-2.6	-0.0	-11.3
3650	13DE1	543G	3	B		8.6	1.9	.77	96.4	93.0	90.0*	33.6	14.	6.5	-2.6	-1.5	-11.6

NO	DATE 196-	TIME CST				MAX MAGN	MAGN RISE	COS Z	BEG HT	MAX HT	END HT	V	VDOT	ER-ROR	LOG MASS	LOG DENS	LOG SIGMA
1	2	3	4	5	6	7	8	9	10	11	12	13	14	15	16	17	18
3653	13DE1	548G	4	B		8.2	2.4	.70	106.2*	101.9*	97.5*	34.7	2.1	11.	-2.3	-1.3	-10.9
3654	13DE1	549G	3	B		8.8	1.8	.77	89.7*	86.7*	83.7*	34.4	15.	27.	-2.7	-0.6	-11.6
3657	13DE1	6 2	3	B		8.8	1.8	.81	86.6*	83.5*	80.4*	27.8	16.	8.3	-2.4	-0.6	-11.6
3664	13DE1	713	3	B		8.3	2.2	.84	86.0*	82.9*	79.7*	25.2	27.	16.	-2.1	-1.2	-11.8
3669	13DE1	726	3	B		7.7	2.5	.85	97.7*	94.5*	91.3*	56.0	38.	36.	-3.0	-1.3	-12.0
3681	13DE1	755	3	B		8.3	2.0	.86	92.2*	89.1*	86.0*	51.1	85.	35.	-3.2	-1.3	-12.3
3895	14DE1	328	3	B		8.5	1.7	.84	101.0*	98.0*	95.1*	25.8	20.	11.	-2.3	-2.6	-11.7
3906	14DE1	4 4	4	B		8.3	2.5	.76	88.5*	84.3*	78.6*	24.5	13.	2.0	-1.8	-0.9	-11.7
3934	14DE1	521	3	B		8.5	2.0	.83	87.7*	84.7*	81.6*	35.6	33.	8.1	-2.7	-0.8	-11.9
3941	14DE1	530	5	B		8.6	2.2	.70	91.5	85.6	80.4*	25.1	13.	1.8	-1.9	-1.2	-11.8
3946	14DE1	535	6	B		8.1	2.2	.79	113.8	104.4	99.0*	38.1	9.3	4.5	-2.2	-2.7	-11.8
3950	14DE1	545G	5	B		8.3	2.1	.78	105.8*	100.4*	95.1*	30.6	14.	2.6	-2.1	-2.6	-11.8
3952	14DE1	557G	3	B		8.2	2.5	.70	95.3	92.0*	89.6*	34.7	5.9	2.6	-2.5	-0.9	-11.2
3953	14DE1	6 0	4	B		8.9	1.5	.83	94.4	89.8	85.2	37.9	16.	6.2	-2.8	-0.8	-11.8
3974	15DE1	413	4	B		8.5	2.3	.71	93.8*	89.7*	85.6*	24.8	16.	4.1	-2.0	-1.7	-11.8
3989	15DE1	5 0	5	B		7.5	2.3	.87	115.3*	110.1*	104.8*	43.7	35.	12.	-2.4	-3.6	-12.1
3994	15DE1	5 7	5	B		8.3	2.3	.73	98.0	92.1	87.4*	32.7	23.	2.3	-2.2	-2.0	-12.0
3996	15DE1	513	3	B		7.4	2.5	.89	106.2	103.4*	101.2	45.5	6.4	16.	-2.7	-1.7	-11.1
4004	15DE1	541	4	B		8.3	2.0	.87	86.9*	86.9*	76.0*	33.3	17.	2.3	-2.3	-0.3	-11.8
4005	15DE1	548	3	B		8.3	2.0	.88	81.3*	78.2*	75.0*	32.4	17.	8.8	-2.5	0.2	-11.6
4006	15DE1	549	5	B		8.2	2.1	.83	100.0*	94.7*	89.3*	37.8	11.	3.4	-2.5	-1.3	-11.7
4008	15DE1	555G	4	B		8.2	2.5	.72	99.3*	92.1	89.5*	34.2	2.9	4.3	-2.2	-0.7	-11.1
4009	15DE1	557G	4	B		8.7	1.9	.71	103.8*	98.8	93.1*	34.0	7.7	2.9	-2.4	-1.8	-11.6
4010	15DE1	558G	4	B		8.6	2.0	.72	98.2	89.4	88.1*	33.1	3.9	2.9	-2.4	-0.8	-11.3
4013	15DE1	620G	3	B		9.3	1.4	.69	96.5	93.3	90.5*	30.4	4.2	15.	-2.7	-0.8	-11.1
4019	15DE1	7 6	4	B		8.6	2.0	.79	87.1*	85.4	76.2*	34.5	36.	3.6	-2.4	-0.7	-12.2
4030	2JA2	11 8	4	B		8.0	2.5	.74	94.4	91.0*	88.5	41.0	.04	40.	-2.7	2.9	-9.0
4038	2JA2	1123	3	B		8.4	2.1	.77	93.4	89.6	86.7	30.9	22.	7.5	-2.4	-1.4	-11.8
4039	2JA2	1124	3	B		8.3	1.6	.82	114.7	111.8	109.9	45.0	67.	43.	-3.1	-3.8	-12.1
4042	2JA2	1219Q	3	B		7.9	2.5	.79	91.7	89.1	87.2	37.6	31.	23.	-2.7	-1.3	-11.8
4046	2JA2	1230	3	B		8.6	1.6	.83	95.7*	92.5*	89.3*	36.4	-1.6	13.	-2.8	0.2	-10.6
4047	2JA2	1230Q	3	B		7.9	2.5	.75	99.0*	96.3*	91.4*	42.2	94.	33.	-2.6	-2.6	-12.5
4137	3JA2	10 2	3	B		8.5	1.8	.81	94.8	91.7	89.2	50.8	20.	16.	-3.3	-0.6	-11.7
4138	3JA2	10 6	4	B		8.6	1.6	.86	95.2*	91.1*	87.0*	28.0	11.	4.2	-2.3	-1.3	-11.5
4140	3JA2	1024	4	B		8.2	1.8	.84	107.0*	102.8*	98.6*	37.1	16.	6.8	-2.5	-2.4	-11.7
4144	3JA2	1112Q	5	B		7.8	2.2	.88	98.9*	98.9*	86.1*	39.7	17.	7.1	-2.3	-1.4	-11.9
4145	3JA2	1113Q	4	B		8.1	2.0	.88	94.3*	90.3*	86.2*	37.1	69.	23.	-2.5	-1.9	-12.3
4146	3JA2	1114	3	B		8.9	1.6	.74	93.9	90.3	87.9*	36.3	30.	8.0	-2.9	-1.4	-11.9
4147	3JA2	1115	4	B		9.3	1.0	.82	92.6*	87.7	81.9*	35.6	23.	5.9	-2.8	-0.8	-12.0
4150	3JA2	1122Q	4	B		8.6	1.4	.88	91.7*	87.7	81.4	39.6	11.	5.7	-2.7	-0.1	-11.6
4151	3JA2	1128	3	B		8.5	1.8	.83	91.3	88.1	85.9	37.1	11.	11.	-2.8	-0.4	-11.4
4152	3JA2	1128	3	B		7.9	2.5	.82	88.6	85.6*	82.6	26.5	19.	2.4	-2.0	-1.2	-11.7
4154	3JA2	1129Q	4	B		8.5	1.6	.86	94.5*	90.5*	86.4*	37.7	28.	5.2	-2.7	-1.2	-11.9
4156	3JA2	1130	3	B		8.8	1.5	.82	89.1	85.7	82.3	27.2	16.	5.8	-2.4	-0.9	-11.6
4157	3JA2	1210Q	4	B		8.9	1.4	.82	96.4*	90.4	85.4*	40.9	14.	4.4	-2.8	-0.9	-11.8
4161	3JA2	1217Q	4	B		7.9	2.3	.81	98.9*	94.1*	89.3*	37.8	-.12	5.5	-2.4	1.6	-9.7
4162	3JA2	1220Q	3	B		8.9	1.6	.81	84.2	81.3	78.5	39.1	44.	21.	-3.0	-0.4	-12.0
4163	3JA2	1228	4	B		9.0	1.2	.83	96.8*	91.4	86.1*	38.8	22.	4.7	-2.8	-1.3	-12.0
4165	3JA2	13 4Q	3	B		8.3	2.4	.72	91.2	88.2	85.3	39.3	11.	13.	-2.7	-0.3	-11.5
4166	3JA2	13 6	3	B		8.8	1.5	.85	83.7	80.5	77.2	30.8	27.	10.	-2.6	-0.4	-11.8

NO	DATE 196-	TIME CST				MAX MAGN	MAGN RISE	COS Z	BEG HT	MAX HT	END HT	V	VDOT	ER-ROR	LOG MASS	LOG DENS	LOG SIGMA
1	2	3	4	5	6	7	8	9	10	11	12	13	14	15	16	17	18
4171	3JA2	1313Q	4	B		8.9	1.6	.70	101.3*	92.2	90.7*	37.7	22.	3.7	-2.6	-1.9	-12.0
4177	3JA2	14 8	3	B		9.2	1.4	.74	92.6	89.6	87.2	24.0	20.	4.1	-2.4	-1.8	-11.7
4187	4JA2	1215Q	4	B		8.2	2.2	.77	97.1	92.4	87.9*	39.9	21.	6.2	-2.6	-1.5	-11.9
4189	4JA2	1222Q	5	B		8.8	1.6	.74	107.3*	106.3	94.5*	41.1	24.	4.8	-2.7	-2.3	-12.1
4197	4JA2	1229Q	3	B		8.6	1.8	.73	102.8*	99.8*	96.8*	39.2	35.	19.	-2.9	-2.4	-12.0
4199	4JA2	13 7Q	4	B		8.1	2.4	.73	93.0	88.6	84.2	38.7	18.	5.5	-2.5	-1.0	-11.9
4207	4JA2	1317Q	4	B		8.7	1.7	.69	107.2*	102.5*	97.8*	39.7	17.	4.4	-2.7	-2.4	-11.9
4217	4JA2	15 1	4	B		8.7	1.6	.85	88.3	84.1	80.0	24.5	.35	1.4	-2.1	1.4	-10.1
4224	4JA2	17 5	3	B		8.4	1.7	.80	111.0*	107.9*	104.7*	18.5	-.45	2.9	-1.7	-2.0	-10.1
4258	15JA2	417	4	B		8.6	1.7	.85	83.0*	78.4*	73.8*	19.8	5.7	1.7	-1.7	-0.2	-11.3
4268	15JA2	513	4	B		9.3	1.1	.68	105.2*	100.9*	96.7*	30.7	20.	6.8	-2.6	-2.7	-11.9
4280	15JA2	622	4	B		9.6	0.5	.83	98.4*	91.0	86.1*	30.0	8.5	4.8	-2.6	-1.0	-11.6
4281	15JA2	624	4	B		7.5	2.5	.84	99.7	93.8*	90.4*	38.4	.69	2.9	-2.2	0.2	-10.4
4303	16JA2	4 1	6	B		8.6	1.5	.84	97.3*	91.1	83.6	30.1	19.	3.4	-2.2	-1.6	-12.0
4304	16JA2	4 7	4	B		8.8	1.5	.84	88.9*	84.8*	80.8*	20.2	8.4	1.8	-1.9	-1.0	-11.4
4305	16JA2	4 9	4	B		7.7	2.4	.80	102.7*	98.4*	94.2*	26.7	5.3	1.2	-1.8	-2.0	-11.3
4330	16JA2	6 9	4	B		9.2	1.2	.78	93.1*	88.6*	84.1*	34.9	8.9	6.9	-2.8	-0.5	-11.5
4331	16JA2	621	4	B		8.4	1.8	.80	96.3*	91.7*	87.2*	28.4	18.	11.	-2.1	-1.9	-11.8
4332	16JA2	623	3	B		8.4	1.8	.83	87.9	85.1	82.9	36.0	2.8	20.	-2.8	0.8	-10.7
4338	16JA2	8 8	4	B		8.9	1.3	.83	95.2	90.3	85.7*	44.5	21.	22.	-3.0	-0.6	-11.9
4340	16JA2	818	3	B		8.8	1.1	.90	82.8	79.9	77.7	36.4	-32.	33.	-3.0	-0.1	-11.8
4347	16JA2	915	4	B		9.5	0.7	.78	98.7	93.7	88.7	38.9	22.	7.6	-3.0	-1.4	-12.0
4351	16JA2	11 5	4	B		8.0	2.2	.79	99.4	95.3	91.6	36.4	32.	10.	-2.4	-2.2	-12.0
4352	16JA2	11 8	4	B		8.8	1.4	.81	94.0	89.7	85.4	36.0	31.	4.9	-2.7	-1.4	-12.0
4353	16JA2	11 8	4	B		8.7	1.7	.80	91.0	85.9	81.3	37.8	12.	6.2	-2.7	-0.2	-11.7
4356	16JA2	1118	3	B		9.5	1.1	.76	84.5	81.8	79.2	34.2	27.	29.	-3.1	-0.2	-11.8
4364	17JA2	917	3	B		7.9	2.0	.86	97.5*	94.4*	91.4*	48.6	30.	48.	-2.9	-1.4	-11.8
4365	17JA2	918	3	B		7.8	2.5	.77	96.2*	93.1*	90.1*	38.0	9.4	3.5	-2.5	-1.1	-11.4
4375	17JA2	1023	3	B		8.5	1.6	.81	99.9*	96.7*	93.5*	37.4	-1.6	22.	-2.8	-0.2	-10.6
4378	17JA2	1129	4	B		8.1	2.5	.68	95.3	91.9*	89.0	36.4	58.	21.	-2.5	-2.1	-12.2
4381	17JA2	1215	4	B		8.2	2.2	.71	104.3	100.4	97.1	37.7	22.	5.3	-2.5	-2.4	-11.9
4382	17JA2	1223	4	B		8.1	2.2	.75	103.1*	98.9*	94.7*	37.8	1.1	4.6	-2.5	-0.3	-10.6
4384	17JA2	1230	4	B		9.4	0.9	.81	89.8*	85.4*	80.9*	23.5	2.7	3.1	-2.3	-0.0	-11.0
4403	18JA2	1310	3	B		9.4	0.8	.80	94.2	91.2	88.7	27.9	21.	4.7	-2.7	-1.7	-11.7
4404	18JA2	1311	4	B		8.1	2.2	.79	92.3*	87.7*	83.1*	29.1	13.	3.5	-2.1	-1.2	-11.7
4408	18JA2	1318	6	B		7.8	2.3	.86	95.2*	88.3*	81.5*	27.5	11.	3.7	-1.7	-1.4	-11.8
4412	18JA2	14 0	5	B		9.0	1.5	.74	98.6	92.5	87.5*	26.2	4.9	2.3	-2.1	-1.3	-11.4
4420	18JA2	14 8	3	B		9.0	1.2	.85	87.8*	84.7*	81.6*	26.6	21.	7.8	-2.5	-1.0	-11.7
4426	18JA2	1429	3	B		8.8	1.5	.78	97.4	94.5	92.3	16.1	2.0	5.0	-1.7	-1.8	-10.6
4427	18JA2	15 1	4	B		8.9	1.1	.87	90.8*	86.2*	81.7*	20.7	1.9	1.3	-1.9	-0.3	-10.8
4428	18JA2	15 4	4	B		8.2	2.1	.80	97.1*	92.3*	87.4*	24.3	5.3	.96	-1.8	-1.5	-11.3
4431	18JA2	1523	4	B		8.7	1.6	.71	101.5*	96.8*	92.2*	21.3	1.3	3.3	-1.8	-1.4	-10.8
4434	18JA2	1527	3	B		8.1	2.0	.85	93.1	90.3	87.8	20.6	7.1	3.1	-1.8	-1.7	-11.2
4478	29JA2	426	3	B		9.3	1.0	.77	97.6*	94.7*	91.9*	21.2	-6.4	11.	-2.3	-1.9	-11.2
4480	29JA2	5 4	5	B		8.7	1.8	.71	100.5*	93.3	88.5*	26.1	1.4	3.3	-2.0	-0.7	-10.9
4498	29JA2	629	4	B		7.8	2.5	.74	99.8	92.4*	89.0*	34.0	.47	1.4	-2.1	0.3	-10.4
4530	30JA2	517	3	B		8.6	1.7	.80	93.2*	90.1*	87.0*	30.1	.33	2.0	-2.5	1.2	-9.9
4546	30JA2	716	3	B		8.9	1.3	.83	89.4*	86.2*	83.0*	33.3	35.	7.7	-2.8	-1.1	-11.9
4549	30JA2	724	4	B		9.1	1.3	.75	90.4*	85.7*	81.0*	24.9	10.	.51	-2.2	-1.0	-11.6
4565	30JA2	11 4	5	B		9.3	0.9	.84	91.9	86.7	81.7	23.2	4.6	1.2	-2.2	-0.6	-11.3

NO	DATE 196-	TIME CST				MAX MAGN	MAGN RISE	COS Z	BEG HT	MAX HT	END HT	V	VDOT	ERROR	LOG MASS	LOG DENS	LOG SIGMA
1	2	3	4	5	6	7	8	9	10	11	12	13	14	15	16	17	18
4578	31JA2	922	3	B	[illegible]	1.1	.78	89.1*	86.1*	83.0*	26.4	7.2	4.5	-2.5	-0.4	-11.3
4566	30JA2	1112	3	B	[illegible]	2.5	.79	88.5	85.7*	83.6	30.4	11.	1.3	-2.3	-0.7	-11.3
4584	31JA2	10 5	4	B	[illegible]	2.3	.86	94.8*	90.2*	85.5*	31.3	1.9	6.7	-2.0	-0.2	-10.8
4586	31JA2	1010	4	B	[illegible]	2.4	.87	97.6*	93.0*	88.4*	40.7	23.	6.4	-2.4	-1.6	-11.9
4591	31JA2	1025	4	B	9.4	0.9	.81	91.5*	87.0*	82.5*	36.1	17.	8.3	-2.9	-0.6	-11.8
4592	31JA2	1026	3	B	9.0	1.1	.86	88.4*	85.2*	81.9*	24.7	12.	3.7	-2.3	-0.9	-11.5
4593	31JA2	1027	4	B	9.0	1.3	.80	92.5*	87.8*	83.0*	32.1	11.	2.4	-2.5	-0.7	-11.6
4594	31JA2	1029	3	B	8.6	1.6	.81	93.2*	90.1*	87.1*	32.8	38.	10.	-2.6	-1.7	-12.0
4596	31JA2	11 5	3	B	8.2	1.9	.80	97.1*	94.0*	90.8*	31.0	-8.2	9.7	-2.4	-1.4	-11.3
4597	31JA2	11 6	4	B	9.6	0.7	.75	99.3*	94.7	88.4*	43.9	-16.	14.	-3.2	-1.0	-11.9
4598	31JA2	1110	3	B	9.1	1.3	.79	88.4*	85.2*	82.1*	27.3	9.7	4.7	-2.5	-0.5	-11.4
4599	31JA2	1115	3	B	7.5	2.5	.86	95.6*	92.3*	89.0*	38.8	11.	5.1	-2.4	-1.1	-11.5
4605	31JA2	1213	3	B	8.6	1.9	.74	91.0	88.4	86.3	41.1	21.	7.1	-3.0	-0.7	-11.6
4610	31JA2	13 4	3	B	9.6	0.8	.75	93.9	90.9	87.8	27.9	3.8	8.4	-2.7	-0.5	-11.0
4611	31JA2	1310	3	B	8.7	1.8	.79	80.9*	77.9*	74.9*	23.1	14.	1.6	-2.1	-0.3	-11.5
4614	31JA2	1322	3	B	9.6	0.8	.74	94.6*	91.6*	88.6*	21.3	4.0	2.2	-2.4	-1.1	-11.0
4635	1FE2	1217	3	B	9.1	1.2	.83	88.1*	84.9*	81.7*	27.1	24.	5.9	-2.5	-1.1	-11.8
4638	1FE2	1218	4	B	8.0	2.4	.77	88.3*	83.5*	78.8*	27.6	14.	1.1	-1.9	-0.9	-11.7
4639	1FE2	1219	4	B	8.7	1.5	.79	99.4*	94.6*	89.8*	31.9	7.5	2.1	-2.4	-1.4	-11.5
4644	1FE2	13 5	4	B	7.7	2.3	.84	96.6*	91.9*	87.2*	29.3	2.4	.96	-1.9	-0.7	-11.0
4652	1FE2	1327	3	B	8.8	1.2	.88	86.8*	83.8*	80.8*	20.1	4.5	14.	-2.0	-0.4	-11.0
4699	12FE2	5 1	3	C	8.2	2.5	.83	97.1*	92.8*	88.5*	34.5	14.	4.9	-2.4	-1.3	-11.7
4711	12FE2	525	3	C	9.6	1.3	.75	95.4	91.3	89.6*	26.1	3.4	6.9	-2.7	-0.8	-10.9
4715	12FE2	6 7	3	C	8.6	2.0	.87	90.9*	87.6*	84.3*	35.2	11.	12.	-2.7	-0.4	-11.5
4717	12FE2	615	6	C	8.5	2.0	.86	96.7*	85.6	81.5*	27.0	1.6	1.0	-1.9	-0.1	-11.0
4718	12FE2	617	4	C	8.9	1.7	.85	98.5*	98.5*	88.5*	36.8	9.4	14.	-2.7	-0.9	-11.6
4719	12FE2	619	3	C	9.3	1.2	.86	90.9	88.4	86.7	37.0	-33.	80.	-3.3	-1.0	-11.7
4726	12FE2	710	5	C	8.8	1.8	.85	103.6*	95.3	90.6*	36.6	18.	8.6	-2.5	-1.9	-11.9
4731	12FE2	716	3	C	10.0	0.8	.84	85.2*	82.2*	79.2*	22.1	19.	6.3	-2.6	-0.8	-11.7
4732	12FE2	721	3	C	9.2	1.6	.84	85.3	82.4	80.2	27.5	6.6	3.8	-2.7	0.1	-11.1
4744	13FE2	327	3	C	9.8	1.1	.78	88.5	84.8	81.8*	20.1	.35	4.3	-2.3	1.1	-10.0
4752	13FE2	4 8	4	C	9.3	1.2	.84	103.8*	96.3	93.5*	29.2	8.9	2.8	-2.5	-2.0	-11.6
4761	13FE2	512	3	C	9.0	1.9	.72	100.3*	99.1	92.9*	28.4	-8.1	6.8	-2.4	-1.8	-11.4
4764	13FE2	520	4	C	8.5	2.2	.79	100.6	96.0	91.4	30.6	15.	1.8	-2.3	-2.2	-11.8
4765	13FE2	522	4	C	8.5	2.5	.72	95.3*	88.5*	84.5*	25.6	2.8	1.5	-1.9	-0.7	-11.1
4766	13FE2	526	4	C	8.3	2.4	.80	104.9	100.8	96.7	31.3	15.	4.1	-2.3	-2.6	-11.7
4772	13FE2	614	4	C	8.8	2.1	.77	89.8	85.9	82.0	23.5	13.	2.5	-2.1	-1.3	-11.6
4787	13FE2	817	3	C	9.2	1.7	.76	88.7	85.9	83.4	38.3	27.	5.6	-3.1	-0.6	-11.8
4796	13FE2	918	4	C	8.5	2.4	.78	96.7*	92.5	87.2	27.9	9.5	1.3	-2.1	-1.4	-11.6
4797	13FE2	924	3	C	8.7	2.3	.76	88.7*	85.5*	82.3*	17.6	2.9	.35	-1.7	-0.8	-10.9
4804	13FE2	10 6	3	C	9.2	1.6	.80	92.2	89.8	87.5	39.0	-18.	32.	-3.2	-0.7	-11.5
4806	13FE2	1015	4	C	9.6	1.3	.81	89.3*	83.5	79.3*	21.3	5.3	2.5	-2.2	-0.4	-11.3
4814	13FE2	1031	4	C	9.0	1.5	.82	107.0	101.2	96.7*	35.0	29.	5.8	-2.7	-2.8	-12.1
4818	13FE2	11 1	4	C	7.9	2.5	.82	113.4	105.8*	103.3*	42.8	-14.	12.	-2.5	-2.9	-11.8
4820	13FE2	11 5	3	C	8.9	2.0	.76	96.9*	93.7*	90.4*	32.6	5.6	24.	-2.7	-0.9	-11.2
4825	13FE2	1119	4	C	8.4	2.5	.74	96.7	91.3*	87.7*	33.3	15.	1.8	-2.3	-1.6	-11.8
4831	13FE2	1127	3	C	8.2	2.5	.82	90.6	87.0*	83.6*	32.2	10.	6.0	-2.4	-0.7	-11.5
4833	13FE2	1130	4	C	8.3	2.5	.79	97.3*	92.9*	88.6*	28.0	20.	2.0	-2.1	-2.1	-11.9
4839	14FE2	814	3	C	8.3	2.1	.88	93.1	90.2	88.1	36.4	-28.	20.	-2.8	-1.4	-11.7
4847	14FE2	922	3	C	9.6	1.4	.76	86.3*	83.4*	80.5*	26.6	24.	10.	-2.7	-0.8	-11.8

NO	DATE 196-	TIME CST				MAX MAGN	MAGN RISE	COS Z	BEG HT	MAX HT	END HT	V	VDOT	ER-ROR	LOG MASS	LOG DENS	LOG SIGMA
1	2	3	4	5	6	7	8	9	10	11	12	13	14	15	16	17	18
4854	14FE2	929	3	C		9.3	1.5	.72	98.4	95.4	92.7	25.9	18.	4.1	-2.5	-2.3	-11.7
4856	14FE2	1013	3	C		9.5	1.1	.84	93.1*	89.7*	86.4*	27.7	1.6	8.7	-2.7	0.2	-10.6
4859	14FE2	1016	4	C		8.6	2.2	.80	89.1	84.7	80.6	31.8	22.	5.8	-2.4	-0.9	-11.9
4865	14FE2	1126	3	C		8.4	2.5	.76	91.9*	87.0*	82.1*	31.7	13.	5.0	-2.3	-0.9	-11.7
4866	14FE2	12 8	3	C		8.3	2.5	.78	99.6*	95.2*	90.8*	36.2	26.	1.6	-2.4	-2.0	-12.0
4877	14FE2	1325	3	C		9.4	1.4	.80	89.7*	86.9*	84.0*	22.8	11.	12.	-2.4	-1.0	-11.4
4892	15FE2	12 5	3	C		8.0	2.5	.80	112.7*	109.5*	106.4*	26.8	-.38	1.3	-2.1	-1.4	-10.0
4894	15FE2	12 7	3	C		9.1	1.7	.81	90.7	87.5	84.3	34.8	29.	7.7	-2.9	-1.0	-11.9
4895	15FE2	12 8	3	C		9.7	1.2	.79	91.1*	87.9*	84.7*	34.2	39.	3.9	-3.1	-1.2	-12.0
4897	15FE2	1214	4	C		8.3	2.5	.78	94.4	88.5*	85.0*	29.2	9.3	1.0	-2.1	-1.3	-11.6
4917	15FE2	1328	4	C		8.4	2.5	.73	97.9*	93.2*	88.0	30.6	21.	5.6	-2.2	-2.0	-12.0
4937	15FE2	1612	4	C		8.7	2.0	.80	101.8*	97.2*	92.6*	17.9	3.5	1.2	-1.6	-2.4	-11.1
4974	26FE2	7 4	3	C		8.2	2.5	.83	85.9	83.2	81.4	31.2	8.4	8.2	-2.5	-0.1	-11.2
5050	28FE2	9 2	5	C		8.3	2.5	.81	96.3*	93.6	84.0*	31.4	19.	2.6	-2.1	-1.5	-12.0
5062	28FE2	925	4	C		8.6	2.5	.71	93.5*	89.5*	85.4*	29.5	19.	2.1	-2.3	-1.4	-11.9
5063	28FE2	10 1	4	C		8.8	1.6	.87	90.3	85.3	80.4*	39.3	10.	6.5	-2.8	0.0	-11.6
5065	28FE2	10 7	4	C		8.8	1.8	.83	93.4	89.4	85.5	31.8	24.	4.2	-2.6	-1.4	-11.9
5067	28FE2	10 9	4	C		8.2	2.5	.80	103.4*	99.4*	95.3*	34.4	-.36	5.0	-2.4	0.2	-10.1
5068	28FE2	10 9	3	C		9.1	1.7	.77	88.3	85.6	83.7	30.6	16.	5.4	-2.8	-0.6	-11.5
5071	28FE2	1011	3	C		8.5	1.8	.88	95.8*	91.6*	87.4*	30.0	17.	2.7	-2.4	-1.5	-11.7
5072	28FE2	1012	4	C		8.8	2.1	.77	89.9*	83.8	78.7*	31.2	19.	2.2	-2.3	-0.8	-11.9
5073	28FE2	1019	4	C		8.7	2.2	.79	89.5*	84.7*	80.0*	29.3	7.5	2.0	-2.3	-0.4	-11.5
5080	28FE2	11 2	3	C		8.9	2.0	.77	90.2	87.7	85.5	26.6	13.	3.2	-2.5	-1.1	-11.4
5081	28FE2	11 4	3	C		8.6	2.2	.80	87.8*	84.4*	80.9*	28.2	20.	3.6	-2.3	-0.9	-11.8
5087	28FE2	1119	4	C		8.7	1.8	.84	95.3*	90.8*	86.4*	42.1	17.	13.	-2.9	-0.8	-11.8
5088	28FE2	1119	4	C		9.1	1.6	.80	91.3	86.7	82.2	33.3	28.	5.6	-2.7	-1.1	-12.0
5093	28FE2	1124	4	C		8.3	2.5	.81	94.6*	91.6*	84.9*	29.2	6.5	1.6	-2.1	-0.8	-11.4
5096	28FE2	12 1	3	C		8.0	2.5	.83	98.8	96.0*	93.1	31.8	37.	7.1	-2.4	-2.5	-11.9
5097	28FE2	12 1	4	C		8.7	2.1	.82	85.5*	80.7*	76.0*	28.2	7.3	4.4	-2.3	0.1	-11.4
5101	28FE2	12 8	4	C		8.3	2.5	.79	96.1*	91.8*	87.5*	35.0	20.	4.1	-2.5	-1.4	-11.9
5130	28FE2	1523	3	C		8.8	1.9	.77	99.0*	95.8*	92.6*	13.5	-1.1	3.9	-1.3	-1.9	-10.5
5202	12MR2	7 5	3	C		9.0	1.9	.80	84.5*	81.4*	78.3*	21.1	7.6	1.7	-2.1	-0.4	-11.3
5204	12MR2	717	4	C		9.2	1.3	.84	92.0	86.1	81.5*	31.4	12.	5.0	-2.6	-0.7	-11.7
5269	13MR2	8 3	4	C		7.9	2.5	.88	91.8*	88.1*	79.8*	37.5	25.	5.3	-2.3	-0.8	-12.1
5270	13MR2	8 9	5	C		8.4	2.0	.88	93.2*	92.6	80.6*	31.2	15.	3.0	-2.2	-0.9	-11.8
5271	13MR2	816	5	C		8.0	2.3	.88	96.1*	90.7*	85.2*	35.1	13.	3.3	-2.3	-1.1	-11.7
5279	13MR2	830	6	C		8.0	2.2	.87	101.9*	95.5*	89.1*	34.9	12.	1.7	-2.2	-1.7	-11.8
5281	13MR2	916	4	C		9.1	1.5	.82	94.6*	90.5*	86.4*	31.9	13.	4.3	-2.7	-1.0	-11.6
5287	13MR2	925	3	C		8.8	1.8	.82	95.4	91.6	88.5	24.2	8.1	5.7	-2.2	-1.4	-11.4
5289	13MR2	928	4	C		8.7	1.9	.85	92.2	88.2	84.3	28.1	25.	4.1	-2.3	-1.4	-11.9
5292	13MR2	1012	4	C		9.4	1.1	.84	100.8*	95.8	90.7*	41.6	26.	9.6	-3.1	-1.5	-12.0
5294	13MR2	1015	5	C		8.7	1.8	.86	86.9*	76.8	74.4*	22.8	6.7	1.3	-1.8	-0.3	-11.5
5297	13MR2	1021	4	C		8.4	2.4	.72	103.2	98.3	93.9*	45.0	16.	13.	-2.8	-1.7	-11.8
5299	13MR2	11 9	3	C		9.4	1.2	.83	87.7*	84.7*	81.7*	31.9	44.	34.	-2.9	-1.0	-12.0
5301	13MR2	1110	3	C		9.0	1.5	.81	96.3*	93.4*	90.6*	33.0	-7.1	20.	-2.8	-0.9	-11.2
5304	13MR2	1116	4	C		8.3	2.4	.76	96.6*	91.8*	87.1*	39.2	6.6	3.4	-2.6	-0.7	-11.4
5306	13MR2	1128	4	C		9.1	1.6	.77	98.9*	93.3	88.1*	37.0	19.	6.4	-2.7	-1.5	-12.0
5316	14MR2	8 8	4	C		8.8	1.6	.88	93.9*	89.4*	84.9*	34.8	15.	4.2	-2.6	-1.0	-11.7
5317	14MR2	8 9	4	C		8.8	1.7	.85	92.7*	88.0*	83.4*	31.2	11.	4.1	-2.5	-0.8	-11.6
5320	14MR2	814	3	C		8.9	2.1	.85	127.3*	124.1*	120.9*	40.9	-8.8	18.	-2.7	-1.9	-11.3

NO	DATE 196-	TIME CST				MAX MAGN	MAGN RISE	COS Z	BEG HT	MAX HT	END HT	V	VDOT	ER-ROR	LOG MASS	LOG DENS	LOG SIGMA
1	2	3	4	5	6	7	8	9	10	11	12	13	14	15	16	17	18
5323	14MR2	828	4	C		9.1	1.7	.77	96.2*	89.9*	83.6*	31.9	-20.	11.	-2.4	-1.5	-12.0
5324	14MR2	829	4	C		8.7	2.0	.78	99.6	92.7	88.9*	45.7	15.	5.0	-2.9	-1.1	-11.8
5325	14MR2	829	5	C		8.5	2.2	.84	92.2*	79.7*	79.7*	26.0	7.0	2.7	-1.9	-0.7	-11.5
5330	14MR2	9 3	4	C		8.4	2.4	.79	91.9*	87.2*	82.6*	28.6	10.	1.0	-2.1	-1.0	-11.6
5331	14MR2	9 9	3	C		8.1	2.5	.79	100.2*	97.1*	94.0*	44.3	-5.9	15.	-2.9	-0.8	-11.2
5334	14MR2	911	3	C		9.5	1.1	.85	92.1*	92.1*	84.6*	32.8	-14.	22.	-2.9	-0.7	-11.6
5344	14MR2	10 6	3	C		9.1	1.3	.86	93.6*	90.6*	87.6*	33.9	-39.	24.	-2.9	-1.6	-12.0
5346	14MR2	1013	5	C		9.1	1.4	.86	94.9	88.8	83.4*	30.6	22.	2.2	-2.5	-1.5	-12.0
5351	14MR2	1023	4	C		9.3	1.5	.78	92.5	85.1	82.2*	32.5	15.	3.4	-2.6	-0.9	-11.8
5352	14MR2	1026	3	C		8.0	2.5	.85	97.2*	93.9*	90.7*	35.3	8.7	15.	-2.5	-1.2	-11.3
5355	14MR2	11 4	4	C		8.4	2.1	.78	117.0	111.9	107.6*	32.0	13.	8.2	-2.3	-3.7	-11.7
5356	14MR2	1114	3	C		9.3	1.4	.79	95.6*	92.5*	89.4*	40.9	33.	14.	-3.2	-1.3	-11.9
5357	14MR2	1115	3	C		9.4	1.6	.79	83.6*	80.7*	77.7*	27.5	22.	10.	-2.7	-0.4	-11.7
5361	14MR2	12 1	3	C		8.3	2.5	.70	104.9*	102.0*	99.1*	39.0	24.	20.	-2.7	-2.5	-11.8
5362	14MR2	12 6	3	C		9.7	1.2	.76	87.6*	84.0	80.0*	29.7	20.	8.2	-2.8	-0.6	-11.8
5366	14MR2	1211	4	C		8.2	2.5	.78	103.4	93.6*	93.6*	34.8	-3.2	4.4	-2.3	-1.3	-11.1
5368	14MR2	1214	3	C		9.1	1.4	.86	93.5*	90.5*	87.4*	27.0	8.2	15.	-2.5	-1.0	-11.3
5370	14MR2	1219	3	C		8.6	1.9	.86	91.4*	88.2*	85.0*	35.0	23.	10.	-2.7	-1.0	-11.7
5397	14MR2	15 5	3	C		9.0	1.9	.74	92.3*	88.8	85.0	21.6	2.9	1.1	-2.0	-0.7	-11.0
5401	15MR2	1149	3	C		9.0	1.6	.84	92.5*	89.6*	86.6*	35.0	-15.	34.	-2.9	-0.8	-11.5
5403	15MR2	12 8	3	C		8.3	2.5	.83	86.0*	83.0*	76.1	29.2	24.	5.4	-2.1	-0.7	-12.0
5426	15MR2	15 0	3	C		8.8	1.9	.87	77.1	74.2	72.0	19.7	7.2	2.0	-2.1	0.2	-11.1
5482	26MR2	6 5	4	C		8.5	2.0	.84	96.1*	91.5*	86.8*	34.6	13.	3.5	-2.5	-1.2	-11.7
5483	26MR2	6 8	3	C		8.5	2.5	.81	79.5	77.0*	75.2	20.9	13.	3.6	-2.1	-0.3	-11.4
5494	26MR2	7 3	3	C		9.1	1.6	.84	86.4*	83.6*	80.8*	28.2	-3.1	14.	-2.6	0.6	-10.8
5496	26MR2	719	3	C		9.9	1.1	.77	86.5	83.5	80.4	29.9	8.0	17.	-3.0	0.1	-11.3
5538	27MR2	6 4	3	C		9.2	1.2	.86	97.6	94.8	92.8	22.1	11.	7.6	-2.4	-2.1	-11.3
5539	27MR2	613	3	C		9.9	0.9	.81	87.1*	84.3*	81.5*	24.0	9.1	14.	-2.7	-0.4	-11.3
5544	27MR2	623	3	C		8.7	1.8	.85	89.5	86.7	84.6	20.8	5.4	6.5	-2.1	-0.9	-11.0
5557	27MR2	817	3	C		8.8	2.1	.77	87.5	84.7	82.9	26.0	35.	13.	-2.5	-1.4	-11.8
5561	27MR2	10 9	3	C		9.0	1.7	.80	94.9*	91.7*	88.4*	38.3	29.	8.3	-3.0	-1.4	-11.9
5566	27MR2	1018	4	C		8.6	1.8	.85	104.0*	99.6*	95.2*	41.1	13.	9.8	-2.8	-1.8	-11.7
5567	27MR2	1018	3	C		7.9	2.5	.85	102.5	98.7*	96.1	37.6	8.4	25.	-2.6	-1.5	-11.3
5568	27MR2	1024	4	C		9.5	1.2	.80	95.5	92.0	88.5	19.2	2.7	1.1	-2.1	-1.1	-10.9
5569	27MR2	1025	4	C		9.3	1.4	.83	88.7*	84.4*	80.0*	19.9	7.7	1.5	-2.0	-0.8	-11.4
5570	27MR2	1025	4	C		8.7	2.0	.83	90.9*	90.9*	81.4*	21.1	1.3	1.8	-1.8	0.1	-10.7
5571	27MR2	1028	3	C		8.8	1.9	.79	98.1*	95.2*	92.3*	42.6	11.	20.	-3.1	-0.9	-11.4
5588	28MR2	1015	3	C		9.3	1.2	.86	90.9*	88.0*	85.0*	41.8	23.	34.	-3.3	-0.4	-11.7
5595	28MR2	1027	4	C		9.1	1.7	.82	83.7*	79.2*	74.6*	34.0	25.	3.5	-2.7	-0.1	-12.0
5597	28MR2	11 5	4	C		8.2	2.5	.82	97.8	93.7	89.5	31.9	22.	2.6	-2.3	-1.9	-11.9
5598	28MR2	11 6	3	C		9.5	1.2	.79	102.2*	98.2*	94.2*	36.6	7.9	14.	-3.0	-1.2	-11.4
5614	29MR2	1147	4	C		8.0	2.5	.87	91.6*	87.1*	82.7*	26.8	6.4	3.5	-1.9	-0.8	-11.3
5620	29MR2	12 4	4	C		8.8	1.6	.81	114.5*	110.1*	105.8*	26.0	-1.0	5.8	-2.2	-2.0	-10.6
5623	29MR2	12 9	4	C		8.3	2.3	.83	96.6*	91.9*	87.2*	31.1	5.3	2.6	-2.2	-1.0	-11.3
5626	29MR2	1215	4	C		9.6	1.3	.76	97.4*	93.4*	89.4*	23.5	18.	4.6	-2.4	-2.1	-11.8
5667	29MR2	1822	3	C		9.3	0.8	.78	78.7*	73.6	70.8*	13.1	3.7	.51	-1.8	-0.0	-11.1
5671	30MR2	1821	6	C		8.8	2.0	.72	101.9*	98.1*	94.4*	16.1	1.6	.60	-1.5	-2.1	-10.7

TABLE 3

Rough Heights (km) of 327 Radar Meteors

M_{max} \ v	10-15	15-20	20-25	25-30	30-35	35-40	40-45	45-50	50-55	55-60 km/sec
5.7-6.9	number			1	3		1			
	M_{max}			5.7	6.5		6.5			
	H_{beg}			96.9	103.9		110.9			
	H_{max}			94.2	99.8		104.0			
	H_{end}			92.5	95.9		96.1			
	H_{mean}			94.5	99.9		103.7			
	$H_{beg}-H_{end}$			4.4	8.0		14.8			
7.0-7.9				6	5	9	5	4		2
				7.6	7.7	7.8	7.7	7.7		7.8
				97.6	96.5	96.7	110.5	98.7		95.8
				93.4	92.3	93.3	105.8	95.3		91.8
				90.2	89.4	88.3	101.8	92.1		88.0
				93.7	92.7	92.8	106.0	95.4		91.9
				7.4	7.1	8.4	8.7	6.6		7.8
8.0-8.9	1	7	20	39	68	46	11	5	2	
	8.8	8.7	8.6	8.5	8.5	8.5	8.5	8.3	8.4	
	99.0	94.4	90.7	94.2	96.0	96.8	98.5	98.3	93.6	
	95.8	90.8	86.8	89.5	91.7	92.6	94.7	94.5	90.4	
	92.6	87.5	83.0	85.6	87.5	88.6	90.1	89.8	87.6	
	95.8	90.9	86.8	89.8	91.7	92.7	94.4	94.2	90.5	
	6.4	6.9	7.7	8.6	8.5	8.2	8.4	8.5	6.0	
9.0-9.9		2	18	25	27	13	5			
		9.4	9.3	9.3	9.2	9.2	9.3			
		92.1	90.6	92.1	93.3	95.0	97.7			
		88.2	86.8	88.3	89.2	91.0	93.5			
		84.2	83.4	84.9	85.2	87.3	89.0			
		88.2	86.9	88.4	89.2	91.1	93.4			
		7.9	7.2	7.2	8.1	7.7	8.7			
10.0-10.9	1		1							
	10.3		10.0							
	78.7		85.2							
	73.6		82.2							
	70.8		79.2							
	74.4		82.2							
	7.9		6.0							

TABLE 5

Deceleration, σ , and Nominal Density for 249 Radar Meteors

M_{max} \ v	10-15	15-20	20-25	25-30	30-35	35-40	40-45	45-50	50-55	55-60 km/sec
5.7-6.9	Number				1					
	M_{max}				6.7					
	$\log_{10}(-\dot{v})$ (km sec^{-2})				1.38					
	$\log_{10}\sigma$ (cgs)				-11.73					
	$\log_{10}\rho_m$ (cgs)				-2.30					
7.0-7.9				4	1	6	3	1		1
				7.8	7.9	7.8	7.6	7.9		7.7
				.98	1.03	1.23	1.71	.96		1.58
				-11.42	-11.34	-11.68	-12.18	-11.53		-11.98
				-1.34	-.68	-1.08	-2.61	-.41		-1.35
8.0-8.9		5	16	35	57	37	7	4	2	
		8.7	8.5	8.5	8.5	8.4	8.7	8.3	8.4	
		.61	.94	1.21	1.26	1.34	1.25	1.65	1.72	
		-11.05	-11.35	-11.66	-11.74	-11.82	-11.82	-12.13	-11.98	
		-1.05	-1.00	-1.25	-1.39	-1.39	-1.26	-1.88	-.95	
9.0-9.9		2	15	17	21	8	4			
		9.4	9.3	9.3	9.2	9.2	9.2			
		.72	1.00	1.21	1.34	1.37	1.51			
		-11.16	-11.41	-11.63	-11.84	-11.94	-12.00			
		-.99	-.98	-1.06	-1.08	-1.30	-1.34			
10.0-10.9	1		1							
	10.3		10.0							
	.57		1.28							
	-11.03		-11.66							
	-1.55		-.81							

TABLE 6

Velocity and Deceleration Distribution for 249 Radar Meteors

$\dot{v}$ \ v	10-15	15-20	20-25	25-30	30-35	35-40	40-45	45-50	50-55	55-60	km/sec
1-3		3	3	3	1						
3-6	1	2	6	2	4						
6-10		2	8	14	9	4		1			
10-15			9	10	19	11	2	1			
15-20			3	12	15	10	2		1		
20-30			2	12	23	18	6				
30-50				3	9	6	3	1		1	
50-100				1		2	1	2	1		
km/sec^2											